Probing the extended space charge by harmonic disturbances

Isaak Rubinstein* and Boris Zaltzman†
Blaustein Institutes for Desert Research, Ben-Gurion University of the Negev, Midreshet Ben-Gurion, 84990, Israel
(Received 27 April 2009; published 21 August 2009)

We assess the possibility of probing the diffuse electric double layer at a permeable charge-selective interface, such as a nonblocking electrode or ion-exchange membrane, under a finite steady-state current-voltage bias by small harmonic high-frequency current-voltage disturbances. Our main conclusion is that for a finite underlimiting bias, the electric double layer at such an interface is not amenable to this kind of probe; the high-frequency response of the system is dominated by the quasielectroneutral bulk. This is similar to the previously studied zero-bias case. On the other hand, the extended space charge in such double layers may be probed in this way both by the linear and nonlinear responses, correspondingly by the method of electric impedance spectroscopy and via the previously described anomalous rectification effect. The latter appears preferable over the former as a potential experimental tool for the study of the extended space charge of a nonequilibrium electric double layer.

DOI: 10.1103/PhysRevE.80.021505 PACS number(s): 82.45.Gj, 82.45.Fk

I. INTRODUCTION

In our recent study [1], we re-examined the electrodiffusion time scales near the equilibrium. The purpose of this re-examination was to assess the possibility of probing the diffuse electric double layer (EDL) at a permeable charge-selective interface, such as that of cathode in cathodic metal deposition, an ion-exchange membrane, or an array of nanochannels, by small harmonic high-frequency current-voltage disturbances (electrical impedance spectroscopy, EIS), an issue first addressed by Macdonald and Franceschetti [2]. Our main conclusion was that the EDL at such interfaces, as opposed to that at a blocking interface, is essentially unamenable to such a probing with the entire system's high-frequency response dominated by the quasielectroneutral bulk. In the current follow-up paper, we address the same question away from equilibrium, under a finite steady-state current-voltage bias, thus following the previous studies by Macdonald and Franceschetti [3]. We particularly focus on the issue of probing the extended space charge forming in such EDLs in binary electrolytes in the course of concentration polarization near the limiting current [4]. This extended space charge is the source of nonequilibrium electrokinetic effects, such as formation of the Dukhin's vortices and non-equilibrium electro-osmotic instability in ionic conductance [5,6]. This makes direct experimental probing of the extended space charge a relevant task. These effects likely control several processes of considerable applied importance, such as overlimiting conductance in electrodialysis and shock formation in protein preconcentration in micro-nanochannel systems [7]. In this regime, corresponding to extreme electrolyte depletion, the classical Poisson-Nernst-Planck description of electrodiffusion is suitable without a need to account for steric effects relevant for high ionic concentrations [8]. The analysis is performed upon the same nonblocking model problems as previously [1]. The conclusion is that, whereas the main features of nonequilibrium analysis hold also for quasiequilibrium at a finite underlimiting bias, extended space charge is amenable to probing via both linear (Sec. II) and nonlinear (Sec. III) system's responses using the EIS technique and the anomalous rectification effect [9]. Until the discovery of the extended space charge electro-osmosis and its related nonequilibrium electro-osmotic instability [5,6], this effect remained the only known macroscopic "footprint" of extended space charge in concentration polarization. It is argued in Sec. III that both these phenomena are expressions of the same feature of extended space charge of nonequilibrium EDL distinguishing it from the common diffuse space charge of quasiequilibrium EDL.

II. ELECTRICAL IMPEDANCE SPECTROSCOPY AND EDL UNDER CURRENT

Below, we analyze the following two model problems. The first model concerns a solution layer flanked by two ideal permselective membranes (ideal nonblocking electrodes). The second problem addresses a three-layer setup modeling the concentration polarization at the nonideal cation-selective membrane/electrolyte layer interface.

The first model reads

$$c_{\pm t} = -j_{\pm x}, \tag{1}$$

$$\varepsilon^2 \varphi_{xx} = c_- - c_+, \tag{2}$$

$$\varphi(0,t) = -\varphi(1,t) = \frac{V}{2} + \frac{\alpha}{2}\cos\,\omega t, \tag{3}$$

$$j(0,t) = j(1,t) = 0, \tag{4}$$

$$c_+(0,t) = c_+(1,t) = N, \tag{5}$$

*robinst@bgu.ac.il
†boris@bgu.ac.il

$$\int_0^1 c_- dx = 1. \tag{6}$$

Here, c_+ and c_- are the dimensionless concentrations of cations and anions, respectively (normalized by the average concentration in the system c_0), φ is the dimensionless electric potential (normalized by the thermal potential kT/e), x is the dimensionless spatial coordinate (normalized by the macroscopic length scale L), t is the dimensionless time (normalized by the macroscopic diffusion time $T=L^2/D$, D is a typical ionic diffusivity in the electrolyte solution, assumed equal for ions of both signs), and j_+ and j_- are the dimensionless ionic fluxes defined as

$$j_\pm = -(c_{\pm x} \pm c_\pm \varphi_x). \tag{7}$$

$N \gg 1$ is the dimensionless fixed charge density in the membranes, V is a constant dimensionless voltage bias applied between the ideal permselective membranes (ideal nonblocking electrodes), and α is a small perturbation parameter. Equation (1) is the ionic mass conservation (Nernst-Planck) equation and Eq. (2) is the Poisson equation with the space charge in the right-hand side due to the local ionic concentration imbalance. Equation (4) asserts impermeability of the membranes for co-ions, Eq. (5) fixes the counter-ion concentration in the membranes equal to the normalized concentration of the fixed charges, whereas the normalization condition (6) specifies the average dimensionless co-ion concentration in the system at unity. Finally, $\varepsilon = l_d/L$ is a crucial dimensionless small parameter in which l_d is the Debye length. Assuming that ε is constant, with the underlying implicit assumption of a constant dielectric permeability, is of course a crude approximation in the current analysis [10] to be relaxed in future studies.

For a binary electrolyte, the expression for the dimensionless total electric current I reads

$$I = -\varepsilon^2 \varphi_{xt} + j_+ - j_-. \tag{8}$$

The first term in the right-hand side of Eq. (8) is the displacement current, whereas the difference of j_+ and j_- forms the conduction current.

For small harmonic perturbations, we seek a solution to the problem (1)–(7) in the following form:

$$c_\pm = c_{0\pm} + \frac{\alpha}{2}[C_\pm(x)e^{i\omega t} + \bar{C}_\pm(x)e^{-i\omega t}], \tag{9}$$

$$\varphi = \varphi_0 + \frac{\alpha}{2}[\Phi(x)e^{i\omega t} + \bar{\Phi}(x)e^{-i\omega t}]. \tag{10}$$

Here, $c_{0\pm}$ and φ_0 are, respectively, the ionic concentrations and the electrical potential for the unperturbed state

$$j_{0-} = 0, \tag{11}$$

$$j_{0+} = I_0 \tag{12}$$

$$\varepsilon^2 \varphi_{0xx} = c_{0-} - c_{0+}, \tag{13}$$

$$\varphi(0,t) = -\varphi(1,t) = \frac{V}{2}, \tag{14}$$

$$c_{0+}(0,t) = c_{0+}(1,t) = N, \tag{15}$$

$$\int_0^1 c_{0-} dx = 1. \tag{16}$$

For the electric current, we have

$$I = I_0\left(1 + \frac{\alpha}{2}(\sigma e^{i\omega t} + \bar{\sigma} e^{-i\omega t})\right), \tag{17}$$

where σ is a complex electrical conductivity (bar referring to a complex conjugate) or admittance, defined as a reciprocal of the electrical impedance $Z(V)$,

$$Z(V,\varepsilon) \overset{\text{def}}{=} \frac{1}{\sigma} = Z_r(V,\varepsilon) + iZ_i(V,\varepsilon). \tag{18}$$

Here, the real part $Z_r = \mathbf{Re}\ Z$ is the resistance and $Z_i = \mathbf{Im}\ Z$ is the reactance.

In Fig. 1(a), we present the impedance complex plane plots calculated numerically for a sequence of voltages. We note the presence of two characteristic branches (Warburg impedance [11] and quasielectroneutral bulk impedance [1]) at equilibrium (curve 1) and quasiequilibrium (curve 2). The characteristic Warburg response in Fig. 1(a) breaks down at low frequencies with the impedance approaching the real line due to classical finite diffusion length effects [12,13]. A further increase of voltage, followed by current saturation and the appearance of extended space charge [see inset of Fig. 1(b)], yields the breakdown of the classical EIS picture and merging of these two characteristic branches [see Fig. 1(a)]. This merging is accompanied by the appearance of an additional intermediate phase-shift maximum at the Bode plot (phase shift versus frequency) [see Fig. 1(b)] located at the frequency $\omega_p = O(\varepsilon^{-4/3})$ corresponding to the $t_p = O(\varepsilon^{4/3})$ time scale. Previously, this time scale was inferred in Ref. [4] in relation to the extended space charge with its characteristic length scale $O(\varepsilon^{2/3})$. We note that at the high-frequency edge $\omega \geq O(\varepsilon^{-2})$ [bottom left corner in Fig. 1(a) and upper right corner in Fig. 1(b)], all curves merge. As previously pointed out for the equilibrium case [1], here also this merging is because in this frequency range system's impedance response is dominated by the capacitance of the quasielectroneutral bulk rather than that of the EDL. The latter remains largely insensitive to disturbances in this frequency range.

As the first test of universality of this observation, we turn to the second model problem addressing a three-layer setup with a nonideal cation-exchange membrane, separating two electrolyte diffusion layers flanked on the outside by two stirred bulks. The corresponding boundary-value problem reads

$$c_{\pm t} = -j_{\pm x}, \quad \varepsilon^2 \varphi_{xx} = Q(x) + c_- - c_+, \tag{19}$$

$$Q(x) = N[H(x-1) - H(x-2)], \tag{20}$$

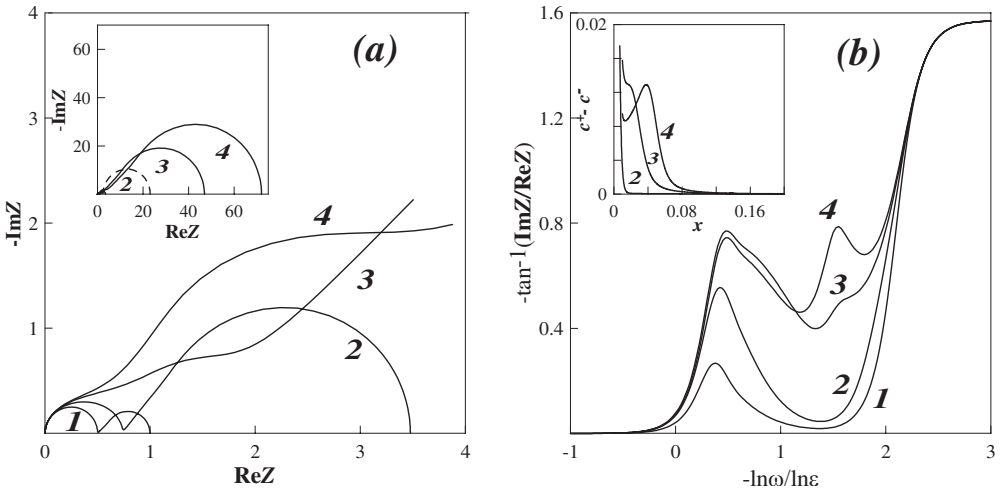

FIG. 1. (a) Impedance complex plane and (b) Bode plots for a one-layer system for a sequence of voltages and $N=20$, $\varepsilon=0.001$. (a) Impedance complex plane (reactance vs resistance) plots for (1) equilibrium EDL $V=0$, (2) quasiequilibrium EDL $V=5$, (3) transition to nonequilibrium EDL (appearance of the extended space charge) $V=15$, (4) nonequilibrium EDL $V=25$. Inset: full-scale plots. (b) Bode (phase shift vs dimensionless frequency) plots for $V=$(1) 0, (2) 5, (3) 15, and (4) 25. Inset: Space charge density vs x-coordinate plots

$$\varphi(0,t) = -\varphi(3,t) = \frac{V}{2} + \frac{\alpha}{2}\cos\,\omega t, \tag{21}$$

$$c_+(0,t) = c_-(0,t) = c_+(3,t) = c_-(3,t) = 1. \tag{22}$$

The dimensionless ionic fluxes are specified by Eq. (7) in the electrolyte layers ($0<x<1$ and $2<x<3$) and equal

$$j_\pm = -D_0(c_{\pm x} \pm c_\pm \varphi_x) \tag{23}$$

inside the membrane ($1<x<2$). Here, $D_0=D_m/D$ is the relative ionic diffusivity inside the membrane, with D_m being the dimensional ionic diffusivity in the membrane assumed equal for both ions. $N>0$ in Eq. (20) is the concentration of fixed charges (negative) in the membrane and $H(x)$ is the Heaviside function; boundary conditions (21) specify the potential drop across the electrolyte layer and conditions (22) fix the concentration at the edges of the electrolyte layer equal to the concentration in the stirred bulk. Similarly to the one-layer models (1)–(7), the solution to the problem (19)–(23) is sought in forms (9) and (10). The suitable linearized problem for the space-dependent amplitudes $C_\pm(x)$ and $\Phi(x)$ is solved numerically.

In Fig. 2, we present the impedance complex plane and Bode plots calculated numerically in the three-layer model (19)–(23) for a sequence of voltages. We note the merging of the two characteristic branches in the impedance complex plane plot at the limiting current. This is accompanied by the

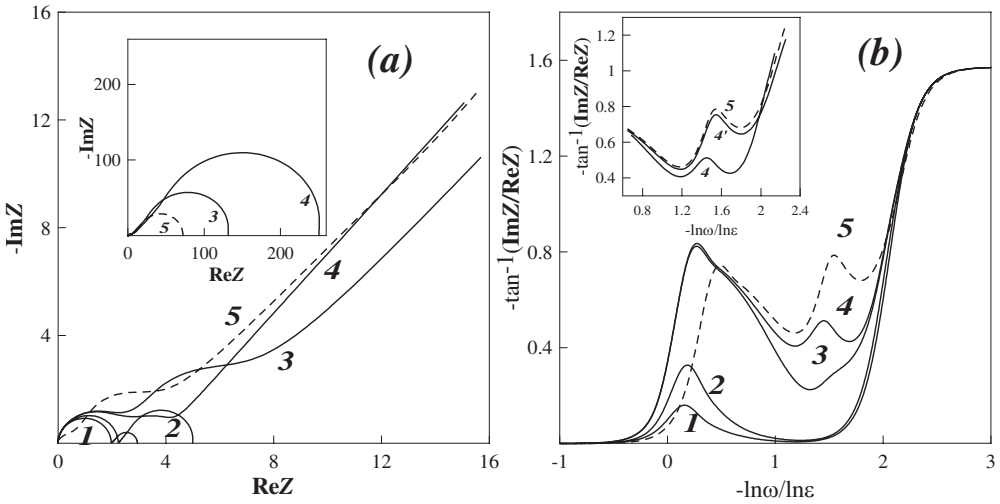

FIG. 2. (a) Impedance complex plane and (b) Bode plots for a three-layer system for a sequence of voltages and $N=20$, $D_m=0.05$, and $\varepsilon=0.001$. (a) Impedance complex plane (reactance versus resistance) plots for (1) equilibrium EDL $V=0$, (2) quasiequilibrium EDL $V=5$, (3) transition to nonequilibrium EDL (appearance of the extended space charge) $V=15$, (4) nonequilibrium EDL $V=25$, and (5) one-layer system $V=25$. Inset: full-scale plots. (b) Bode (phase shift vs dimensionless frequency) plots for $V=$(1) 0, (2) 5, (3) 15, (4) 25, and (5) one-layer system $V=25$. Inset: enlarged high-frequency range of nonequilibrium phase-frequency plots 4 and 5 with added plot 4′ corresponding to the potential drop of curve 4 recalculated for the depleted diffusion layer only.

appearance of an intermediate phase maximum in the Bode plots [Fig. 2(b)] at the characteristic extended space charge frequency $\omega_p = O(\varepsilon^{-4/3})$ that we previously observed in the one-layer model and that is related to the extended space charge length scale $O(\varepsilon^{2/3})$. The relative decrease of the amplitude of this maximum results from the shielding of the depleted diffusion layer by the high resistance of the ion-exchange membrane. This is illustrated in the inset of Fig. 2(b), where phase-frequency plots for the one- and three-layer setups are complemented by the plot in which the voltage response to current perturbations of curve 4 is recalculated for the depleted diffusion layer only (curve 4′). The overall conclusion of this section is that the two observed effects of branch merging in the impedance complex plane plot and the appearance of an intermediate phase-shift maximum in the Bode plot should make the extended space charge amenable to an accurate electrical impedance spectroscopy study. However, in practical terms, this might be quite a formidable task due to the aforementioned shielding effect.

III. NONEQUILIBRIUM EDL AND ANOMALOUS RECTIFICATION

In this section, we study the possibility of probing the extended space charge via a nonlinear response to harmonic disturbances. Specifically, we address the possibility of such a probing via the anomalous rectification effect. This effect was previously predicted from a numerical study of a one-layer model and was observed experimentally in cathodic deposition from a copper sulfate solution [9]. The term "anomalous" refers to the increase of the dc current component upon the application of an ac voltage modulation in a suitable high-frequency range at the limiting current of a steady-state voltage-current curve. This increase is counterintuitive (anomalous) in terms of quasistatic reasoning for a convex V-C curve. Below, we analyze this effect analytically in a one-layer model with the results compared to those obtained numerically for a three-layer model. We begin by analyzing the one-layer problem (1)–(7) for a solution layer flanked by two ideal permselective membranes (ideal nonblocking electrodes).

We seek a solution to Eqs. (1)–(7) in the from

$$c_\pm = c_{0\pm} + \frac{\alpha}{2}(C_\pm e^{i\omega t} + \bar{C}_\pm e^{-i\omega t}) + \alpha^2(C_{\pm,22}e^{2i\omega t} + \bar{C}_{\pm,22}e^{-2i\omega t} + C_{\pm,20}), \tag{24}$$

$$\varphi = \varphi_0 + \frac{\alpha}{2}(\Phi e^{i\omega t} + \bar{\Phi} e^{-i\omega t}) + \alpha^2(\Phi_{22}e^{2i\omega t} + \bar{\Phi}_{22}e^{-2i\omega t} + \Phi_{20}), \tag{25}$$

$$I = I_0 + I_0\frac{\alpha}{2}(\sigma e^{i\omega t} + \bar{\sigma} e^{-i\omega t}) + \alpha^2(I_{22}e^{2i\omega t} + \bar{I}_{22}e^{-2i\omega t} + I_{20}), \tag{26}$$

while keeping the terms quadratic in the voltage perturbation amplitude α and dropping the cubic and higher-order terms in the asymptotic expansions, thus setting a natural accuracy limit for the current analysis. Here, the leading-order terms $c_{0\pm}$, φ_0, and I_0 are once more the ionic concentrations, the electrical potential, and the electric current density in the unperturbed steady state (11)–(16). Spatial amplitudes $C_\pm(x)$, $\Phi(x)$, and σ of the next-order linear correction terms are solutions to the following linearized problem:

$$i\omega C_\pm = -j_{1\pm x}, \tag{27}$$

$$j_{1\pm} = -(C_{\pm x} \pm c_{0\pm}\Phi_x \pm C_\pm \varphi_{0x}), \tag{28}$$

$$\sigma I_0 = -i\omega\varepsilon^2\Phi_x + j_{1+} - j_{1-}, \tag{29}$$

$$x = 0: C_+ = 0, \quad j_{1-} = 0, \quad \Phi = \frac{1}{2}, \tag{30}$$

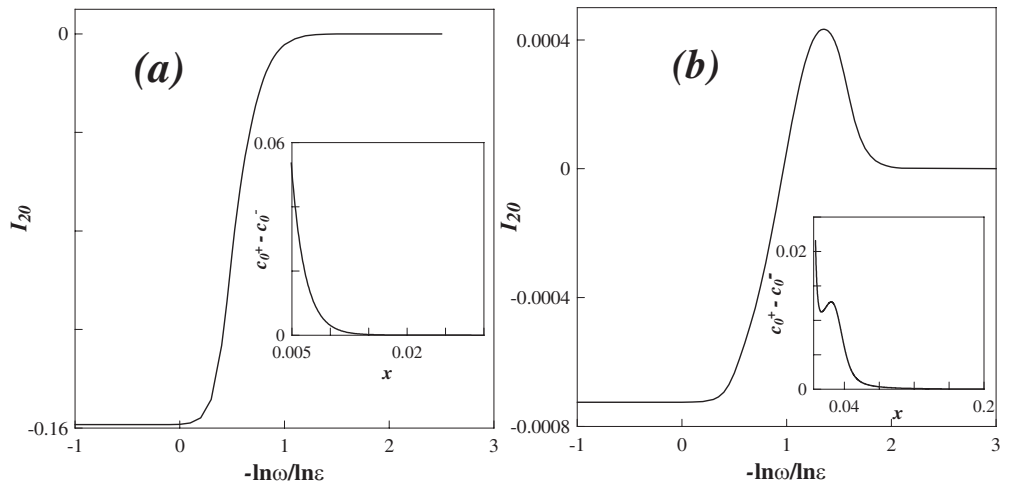

FIG. 3. Calculated dependence of the relative-rectification effect on the dimensionless modulation frequency for $\varepsilon = 0.001$ and (a) quasiequilibrium EDL, $V = 4$, (b) nonequilibrium EDL, $V = 18$. Inset: dimensionless space charge density vs x-coordinate plots

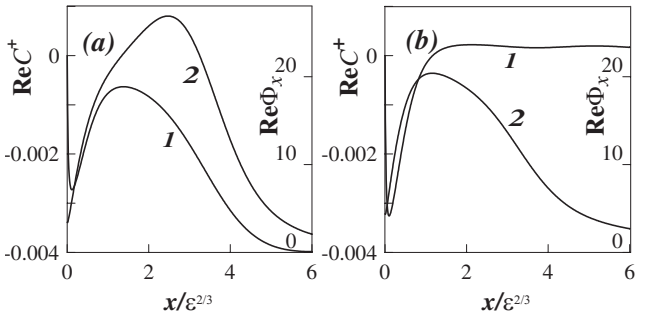

FIG. 4. Calculated first-order corrections to cation concentration C_+ (curve 1) and electric field Φ_x (curve 2) vs scaled spatial variable $x/\varepsilon^{2/3}$ for (a) $\omega=\varepsilon^{-1/3}=10$ and $\omega=\varepsilon^{-4/3}=10000$, $\varepsilon=0.001$, and $V=18$.

$$x=1:C_+=0, \quad j_{1-}=0, \quad \Phi=-\frac{1}{2}. \tag{31}$$

Finally, the spatial amplitudes of the quadratic terms $C_{20,\pm}(x)$, $\Phi_{20}(x)$, and I_{20} are solutions to the following problem:

$$C_{20+x}+c_{0+}\Phi_{20x}+C_{20+}\phi_{0x}+2\,\mathbf{Re}(C_+\Phi_x)=I_{20}, \tag{32}$$

$$C_{20-x}-c_{0-}\Phi_{20x}-C_{20-}\phi_{0x}-2\,\mathbf{Re}(C_-\Phi_x)=0, \tag{33}$$

$$\varepsilon^2\Phi_{20xx}=C_{20-}-C_{20+}, \tag{34}$$

$$x=0,1: \quad C_{20+}=0, \quad \Phi_{20}=0; \quad \int_0^1 C_{20-}dx=0. \tag{35}$$

In Fig. 3, we present the calculated dependence of the relative rectification effect on the modulation frequency for different states of EDL. We note that with the appearance of extended space charge, the current increment changes its sign from negative (conventional rectification) to positive (anomalous rectification). The essence of this phenomenon is rooted in the following peculiarity of the extended space charge compared to that of a quasiequilibrium EDL. The structure of the latter is governed by the following Boltzmann relations:

$$c_+=Ne^{\varphi(0)-\varphi}, \tag{36}$$

$$c_-=\bar{c}e^{\bar{\varphi}-\varphi}, \tag{37}$$

where $\bar{c}$ and $\bar{\varphi}$ are, respectively, the perturbed electroneutral ionic concentration and the electric potential at the depleted membrane-solution interface. Linearizing these equations, we find that

$$\Phi(0)-\bar{\Phi}=-\int_{\mathrm{EDL}}\Phi_x dx=\frac{\bar{C}}{\bar{c}_0}. \tag{38}$$

Here, $\bar{c}_0$ and $\bar{C}$ are the corresponding unperturbed quasielectroneutral interface concentration and its leading-order perturbation. Furthermore, $\bar{\Phi}$ and $\Phi(0)$ are, correspondingly, the values of the leading-order perturbations of the electric potential at the outer quasielectroneutral edge of the EDL and its inner edge at the membrane-solution interface. Equation (38) implies the decrease of the average electric field in the EDL upon the increase of the interface ion concentration. In terms of harmonic perturbations, this means that the first-order correction to the cation concentration C_+ is in a counterphase with that of the electric field Φ_x. This yields a negative correction to the dc current [see Eq. (32)].

In the extended space charge region, the co-ion concentration vanishes, Eqs. (36) and (37) cease to hold, and the electric field is obtained from integration of the Poisson equation

$$\varepsilon^2\phi_{xx}=-c_+. \tag{39}$$

In the extended space charge region, as opposed to the quasiequilibrium EDL, the increase of the local counter-ion concentration yields an increase of the charge density. According

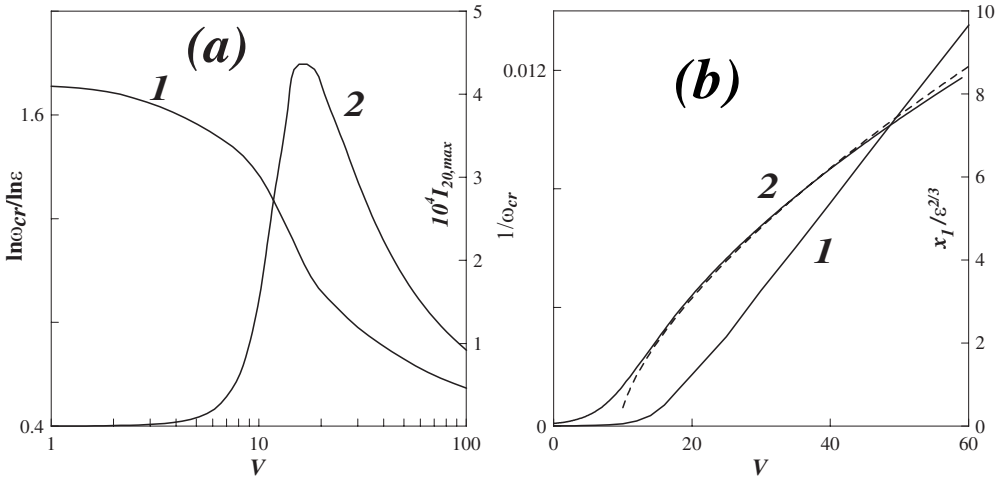

FIG. 5. (a) Critical frequency (curve 1) and maximal current correction (curve 2) vs applied voltage, $\varepsilon=0.001$. (b) Characteristic time (curve 1) and EDL thickness [calculated curve 2, continuous line, theoretically predicted—see Eq. (3.71) of Ref [6]].—curve 2, dashed line] vs applied voltage, $\varepsilon=0.001$.

to the Poisson equation (39), this also yields an increase of the electric field. In terms of harmonic perturbations, this means the first-order correction to the cation concentration C_+ is in phase with that of the electric field Φ_x. This implies a positive contribution to the dc current [see Eq. (32)] resulting in the anomalous rectification effect. We note that this effect reaches a maximum at the extended space charge frequency $\omega_p = O(\varepsilon^{-4/3})$. (The very same peculiarity of the extended space charge response to the external concentration-current density perturbation stands behind the dynamic mechanism of nonequilibrium electro-osmotic instability [6]). This mechanism of anomalous rectification is illustrated in Fig. 4 where we plot the suitably scaled spatial dependence of the amplitudes of the linear corrections C_+ and Φ_x. We note that for the low frequencies [Fig. 4(a)], both corrections are in a counterphase whereas for frequencies in the extended space charge range $\omega_p = O(\varepsilon^{-4/3})$ [Fig. 4(b)], these corrections are in phase in the nonequilibrium portion of the EDL ($x > \varepsilon^{2/3}$).

In Fig. 5(a), we present the voltage dependence of the critical frequency (at which the rectification effect changes from common negative to anomalous positive curve 1) and of the maximal rectified current increment (curve 2). We note that the rectified current value saturates with the completed formation of the extended space charge. A further increase of voltage yields an extension of the anomalous rectification frequency range along with a decrease of the critical frequency. In Fig. 5(b), we present the voltage dependence of the characteristic time (reciprocal of the critical frequency, curve 1) and of the width of the extended space charge zone (essentially identical with the overall thickness of the nonequilibrium EDL) curve 2, calculated numerically (continuous line) and evaluated analytically in Ref. [6] (dashed line). We note [Fig. 5(b)] the linear dependence of the characteristic time on the voltage applied. In Fig. 5(b), we also present the nonequilibrium EDL thickness as a function of the applied voltage, theoretically predicted (dashed line 2) and computed numerically (continuous line 2). Finally, in Fig. 6, we compare these results, obtained for the one-layer model (1)–(7) with those computed numerically for a three-layer one (19)–(23). We note the decrease of critical frequencies for the three-layer versus one-layer case.

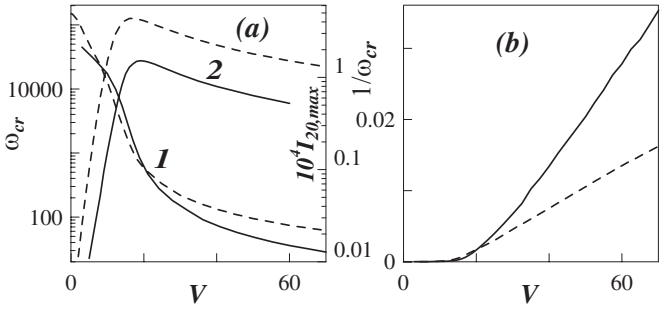

FIG. 6. (a) Voltage dependence of the critical frequency (curve 1) and maximal current rectification (curve 2) vs applied voltage for the three-layer model (continuous lines) compared to those in the one-layer model (dashed lines), $\varepsilon = 0.001$. (b) Voltage dependence of characteristic time in the three-layer model (continuous line) compared to that in the one-layer model (dashed line), $\varepsilon = 0.001$.

Summarizing our findings in this report, the overall conclusion is that the anomalous rectification with its characteristic change of sign of the dc current increment in a suitable frequency range potentially constitutes a more robust and reliable tool for experimental study of the extended space charge in concentration polarization than a more subtle linear EIS.

ACKNOWLEDGMENT

The work was supported by the Israel Science Foundation (Grant No. 65/07).

[1] I. Rubinstein, B. Zaltzman, A. Futerman, V. Gitis, and V. Nikonenko, Phys. Rev. E **79**, 021506 (2009).
[2] J. R. Macdonald, Phys. Rev. **92**, 4 (1953); J. R. Macdonald and D. R. Franceschetti, J. Chem. Phys. **68**, 1614 (1978).
[3] D. R. Franceschetti and J. R. Macdonald, J. Appl. Phys. **50**, 291 (1979); J. Electroanal. Chem. **100**, 583 (1979).
[4] B. M. Grafov and A. A. Chernenko, Dokl. Akad. Nauk SSSR **146**, 135 (1962); W. H. Smyrl and J. Newman, Trans. Faraday Soc. **63**, 207 (1967); R. P. Buck, J. Electroanal. Chem. **46**, 1 (1973); I. Rubinstein and L. Shtilman, J. Chem. Soc., Faraday Trans. 2 **75**, 231 (1979); A. V. Listovnichy, Elektrokhimiya **25**, 1651 (1989); V. V. Nikonenko, V. I. Zabolotsky, and N. P. Gnusin, Sov. Electrochem. **25**, 262 (1989); J. A. Manzanares, W. D. Murphy, S. Mafe, and H. Reiss, J. Phys. Chem. **97**, 8524 (1993); K. T. Chu and M. Z. Bazant, SIAM J. Appl. Math. **65**, 1485 (2005).
[5] I. Rubinstein and B. Zaltzman, Phys. Rev. E **62**, 2238 (2000); S. M. Rubinstein, G. Manukyan, A. Staicu, I. Rubinstein, B. Zaltzman, R. G. H. Lammertink, F. Mugele, and M. Wessling, Phys. Rev. Lett. **101**, 236101 (2008); H.-C. Chang and G. Yossifon, Biomicrofluidics **3**, 012001 (2009); S. S. Dukhin, Adv. Colloid Interface Sci. **35**, 173 (1991); S. S. Dukhin, N. A. Mishchuk, and P. B. Takhistov, Colloid J. USSR **51**, 616 (1989); S. J. Kim, Y. C. Wang, J. H. Lee, H. Jang, and J. Han, Phys. Rev. Lett. **99**, 044501 (2007); Y. Ben and H.-C. Chang, J. Fluid Mech. **461**, 229 (2002); G. Yossifon and H.-C. Chang, Phys. Rev. Lett. **101**, 254501 (2008).
[6] B. Zaltzman and I. Rubinstein, J. Fluid Mech. **579**, 173 (2007).
[7] R. B. Schoch, J. Y. Han, and P. Renaud, Rev. Mod. Phys. **80**, 839 (2008); A. Mani, T. A. Zangle, and J. G. Santiago, Langmuir **25**, 3898 (2009); T. A. Zangle, A. Mani, and J. G. Santiago*ibid.* **25**, 3909 (2009).
[8] S. W. Kenkel and J. R. Macdonald, J. Chem. Phys. **81**, 3215 (1984); M. S. Kilic, M. Z. Bazant and A. Ajdari, Phys. Rev. E **75**, 021502 (2007); **75**, 021503 (2007).
[9] I. Rubinstein, I. Rubinstein, and E. Staude, PCH, PhysicoChem. Hydrodyn. **6**, 789 (1985); I. Rubinstein, *Electrodiffu-*

sion of Ions, 1st ed. (SIAM, Philadelphia, PA, 1990).
[10] J. R. Macdonald and C. A. Barlow, Jr., J. Chem. Phys. **36**, 3062 (1962).
[11] E. Warburg, Ann. Phys. Chem. **67**, 493 (1899); Ann. Phys. **311**, 125 (1901); J. E. B. Randles, Discuss. Faraday Soc. **1**, 11 (1947).
[12] J. R. Macdonald, J. Electroanal. Chem. **53**, 1 (1974).
[13] Warburg segment is more pronounced at higher voltages due to the overall impedance growth in the low frequency due to concentration polarization of the electroneutral bulk.